Does the counterpart of $X(3872)$ in Bottomonium sector exist?

Zhi-Yong Zhou
Collaborators: Dian-Yong Chen and Zhiguang Xiao

Southeast University

October 20th, 2018

Outline

Motivation

Uniqueness of $X(3872)$, right on the $D^0\bar{D}^{0*}$ threshold
$M_{X(3872)} = 3871.69 \pm 0.17$ MeV, $\Gamma_{X(3872)} < 1.2$ MeV
Understandings:

- Meson-exchange model
- Effective Field theory
- Tetraquark model
- Mixing mechanism of $c\bar{c}$ and continua
- $\cdots\cdots$

see Reviews:

F.-K. Guo, C. Hanhart, U.-G. Meiner, Q. Wang, Q. Zhao, and B.-S. Zou, Rev. Mod. Phys. 90, 015004 (2018)

H.-X. Chen, W. Chen, X. Liu, and S.-L. Zhu, Phys. Rept. 639, 1 (2016)

Motivation

Where is its counterpart in Bottomonium sector? Predictions:

- Meson-exchange model
  10562 MeV Tornqvist, Phys. Rev. Lett. 67, 556 (1991), Z. Phys. C61, 525 (1994)
  10561 MeV Swanson, Phys. Rept. 429, 243 (2006)
  10585 MeV Karliner and Nussinov, JHEP 07, 153 (2013)
  qualitative prediction Karliner and Rosner, Phys. Rev. Lett. 115, 122001 (2015)
- Effective Field theory
  10604 MeV in an unpublished version AlFiky, Gabbiani, and Petrov, Phys. Lett. B640, 238 (2006)

Meson exchange models depend on cutoff and exchanged meson. EFT seems to be not sufficient to give a reliable prediction.

Experiment efforts

CMS $\Upsilon\pi^+\pi^-$ S. Chatrchyan et al. (CMS), Phys. Lett. B727, 57 (2013)

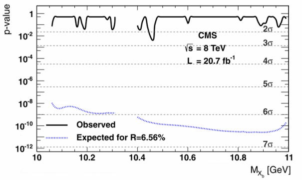

Fig. 3. Observed (solid curve) and expected for $R = 6.56\%$ (dotted curve) local p-values, as a function of the assumed X_b mass.

Belle $\Upsilon\pi^+\pi^-\pi^0$ X. H. He et al. (Belle), Phys. Rev. Lett. 113, 142001(2014)

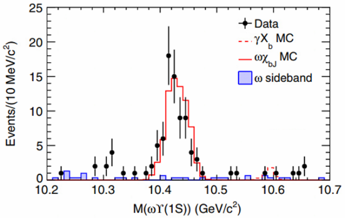

Motivation

The Extended Friedrichs Scheme, dynamical mixing mechanism with a solid mathematical foundation

Xiao and Zhou, J. Math. Phys. 58, 072102(2017)

Xiao and Zhou, J. Math. Phys. 58, 062110(2017)

Xiao and Zhou, Phys. Rev. D 94, 076006 (2016)

What did the Extended Friedrichs Scheme do?

- the mass and width of $X(3872)$
- the isospin breaking effects of of $X(3872)$
- other first excited P-wave states
- there is only one free parameter in these calculations

Zhou and Xiao, Phys. Rev. D96, 054031 (2017), [Erratum: Phys. Rev. D 96, 099905 (2017)]

Zhou and Xiao, Phys.Rev. D97 (2018) no.3, 034011

Prediction power?

Gamow state and mathematical background

Gamow state, a state with a complex eigenvalue, introduced by Gamow to describe nuclear α decay. G.Gamow , Z.Phys. 51 (1928) 204-212

In conventional QM, due to Hermitian of the Hamiltonian, its eigenvalue is real.

Rigged Hilbert Space (RHS) scheme, developed by Bohm and Gadella, provides a solid mathematical foundation for the unstable state.

A.Bohm, M.Gadella, Dirac kets, Gamow vectors, and Gelfund Triplets, Springer Lectures Notes in Physics Vol.348, Springer, Berlin

One of the properties of Gamow states:

$$\begin{aligned} H|z_R\rangle &= z_R|z_R\rangle \\ \langle z_R|H &= z_R^*\langle z_R| \\ \langle z_R|z_R\rangle &= 0 \end{aligned} \tag{1}$$

$|z_R\rangle$ is not a state in Hilbert space but in RHS.

[Friedrichs, Commun. Pure Appl. Math.,1(1948),361]

A free Hamiltonian H_0 with a simple continuous spectrum, $\mathbb{R}^+ \equiv [0, \infty)$, plus a discrete eigenvalue ω_0 ($\omega_0 > 0$). An interaction V between the continuous and discrete parts is produced so that the discrete state of H_0 is dissolved in the continuous spectrum and a resonance is produced.

$$H_0|1\rangle = \omega_0|1\rangle, H_0|\omega\rangle = \omega|\omega\rangle. \tag{2}$$

The free Hamiltonian is then

$$H_0 = \omega_0|1\rangle\langle 1| + \int_0^\infty \omega|\omega\rangle\langle\omega|\mathrm{d}\omega, \tag{3}$$

and the interaction V is written as

$$V = \lambda \int_0^\infty [f(\omega)|\omega\rangle\langle 1| + f(\omega)^*|1\rangle\langle\omega|]\mathrm{d}\omega\,. \tag{4}$$

The eigenvalue problem of $H = H_0 + V$ is exactly solvable.

The Friedrichs Model

[Friedrichs, Commun. Pure Appl. Math.,1(1948),361] solve the eigenstate $|\Psi(x)\rangle$ of $H = H_0 + V$ with eigenvalue x,

$$H\Psi(x) = x|\Psi(x)\rangle. \tag{5}$$

Since $|1\rangle$ and $|\omega\rangle$ form a complete set, the eigenstate $|\Psi(x)\rangle$ can be expressed in terms of $|1\rangle$ and $|\omega\rangle$,

$$|\Psi(x)\rangle = \alpha(x)|1\rangle + \int_0^\infty \psi(x,\omega)|\omega\rangle \mathrm{d}\omega. \tag{6}$$

Note that here $|\Psi\rangle$ is a vector in $\Phi^\times$, and it only make senses as an anti-linear functional on vector $|\phi\rangle \in \Phi$, $\langle\phi|\Psi\rangle$. So, $\psi(x,\omega)$ should be treated as a distribution. Substituting (6) into Eq.(5), one can obtain the following relations:

$$\begin{aligned} (\omega_0 - x)\alpha(x) + \lambda \int_0^\infty f(\omega)\psi(x,\omega)\mathrm{d}\omega &= 0, \\ (\omega - x)\psi(x,\omega) + \lambda f(\omega)\alpha(x) &= 0. \end{aligned} \tag{7}$$

The Friedrichs Model

[Friedrichs, Commun. Pure Appl. Math.,1(1948),361]

Then, for real $x > 0$, we have

$$\psi_{\pm}(x,\omega) = -\tfrac{\lambda\alpha(x)f(\omega)}{\omega - x \pm i\epsilon} + \gamma(\omega)\delta(\omega - x)\,,$$

$$(\omega_0 - x)\alpha_{\pm}(x) + \lambda f(x)\gamma(x) - \alpha_{\pm}(x)\lambda^2 \textstyle\int_0^\infty \tfrac{|f(\omega)|^2}{\omega - x \pm i\epsilon}\mathrm{d}\omega = 0. \qquad (8)$$

one can define

$$\eta^{\pm}(x) = x - \omega_0 - \lambda^2 \int_0^\infty \frac{|f(\omega)|^2}{x - \omega \pm i\epsilon}\mathrm{d}\omega\,, \qquad (9)$$

and analytically continue $\eta^{\pm}$ to the complex plane $\eta(x)$, and η^+ and η^- are the boundary functions of $\eta(x)$ on the upper rim and lower rim of the cut on the positive axis, respectively.

Resonance state

If $\eta(x) = 0$ has a pair of complex conjugate solutions $z_R \in \mathbb{C}_-$ and $z_R^* \in \mathbb{C}_+$ on the second sheet, the right eigenstates for eigenvalue z_R and z_R^* can be expressed as

$$|z_R\rangle = N_R\Big(|1\rangle + \lambda\int_0^\infty \mathrm{d}\omega \frac{f(\omega)}{[z_R-\omega]_+}|\omega\rangle\Big),$$
$$|z_R^*\rangle = N_R^*\Big(|1\rangle + \lambda\int_0^\infty \mathrm{d}\omega \frac{f(\omega)}{[z_R^*-\omega]_-}|\omega\rangle\Big), \tag{10}$$

which are the Gamow states satisfying $H|z_R\rangle = z_R|z_R\rangle$ and $H|z_R^*\rangle = z_R^*|z_R^*\rangle$.

Bound state

If $\eta(x) = 0$ have a solution on the negative real axis on physical Riemann sheet, it represents a bound state. The bound state with eigenvalue z_B can then be represented as

$$|z_B\rangle = N_B\left(|1\rangle + \lambda \int_0^\infty \frac{f(\omega)}{z_B - \omega}|\omega\rangle \mathrm{d}\omega\right) \tag{11}$$

where $N_B = (\eta'(z_B))^{-1/2} = (1 + \lambda^2 \int d\omega \frac{|f(\omega)|^2}{(z_B-\omega)^2})^{-1/2}$.

Virtual state

If $\eta(x) = 0$ has a solution on the negative real axis of the second Riemann sheet, it corresponds to a virtual state.
For the simple virtual poles, similar to resonant states, there are two kinds of states, $|z_v^+\rangle$ by analytical continuation from the upper rim and $|z_v^-\rangle$ lower rim of the cut to the second sheet

$$|z_v^{\pm}\rangle = N_v^{\pm}\Big(|1\rangle + \lambda\int_0^\infty \frac{f(\omega)}{[z_v - \omega]_\pm}|\omega\rangle \mathrm{d}\omega\Big), \quad \langle\tilde{z}_v^{\pm}| = \langle z_v^{\mp}|\,, \tag{12}$$

where $N_v^- = N_v^{+*} = (\eta'^+(z_v))^{-1/2} = (1+\lambda^2\int d\omega \frac{|f(\omega)|^2}{[(z_v-\omega)_+]^2})^{-1/2}$.

The Extended Friedrichs Scheme

For a specific total angular momentum, the interaction between a discrete state $|0\rangle$ having a bare energy eigenvalue m_0, and some continuum two-particle states $|E; n, SL\rangle$, where E is the bare energy eigenvalue in the center of mass system (c.m.s) and n, S, L denote the species, total spin and total orbital angular momentum, respectively, can be expressed in the form of Friedrichs model

$$\begin{aligned} H =& m_0|0\rangle\langle 0| + \sum_{n,S,L} \int_{E_{th,n}}^{\infty} \mathrm{d}E\, E|E; n, SL\rangle\langle E; n, SL| \\ &+ \sum_{n,S,L} \int_{E_{th,n}}^{\infty} \mathrm{d}E f_{SL}^{n}(E)|0\rangle\langle E; n, SL| + h.c. \end{aligned} \tag{13}$$

The Extended Friedrichs Scheme

could be expressed as

$$S_{fi}(E,E') = \delta(E-E')\Big(\delta_{fi} - 2\pi i \frac{f_i(E) f_f{}^*(E)}{\eta^+(E)}\Big). \tag{14}$$

where the resolvent $\eta^{\pm}(x)$ is defined as

$$\eta^{\pm}(x) = x - m_0 - \sum_{n,S,L} \int_{E_{n,th}}^{\infty} \frac{|f^n_{SL}(E)|^2}{x - E \pm i0} \mathrm{d}E\,. \tag{15}$$

the coupling form factor between $|A\rangle$ and $|BC\rangle$ in the Friedrichs model by $f_{SL}(E) = \sqrt{\mu p}\mathcal{M}^{SL}(p)$

The Extended Friedrichs Scheme

The definition of the meson mock state here reads

$$|A(n_r, {}^{2s+1}l_j)(\vec{P})\rangle = \sum_{m_l, m_s} \langle l m_l s m_s | j m\rangle \int \mathrm{d}^3 p\, \psi_{n_r l m_l}(\vec{p})$$
$$\times\, \chi^{12}_{s m_s}\, \phi^{12}\, \omega^{12} \Big| q_1\Big(\frac{m_1}{m_1+m_2}\vec{P}+\vec{p}\Big)\bar{q}_2\Big(\frac{m_2}{m_1+m_2}\vec{P}-\vec{p}\Big)\Big\rangle.$$

χ^{12}, ϕ^{12} and ω^{12} are the spin wave function, flavor wave function and the color wave function, respectively. p_1 (p_2) and m_1 (m_2) are the momentum and mass of the quark (anti-quark). $\vec{P} = \vec{p}_1 + \vec{p}_2$ is the momentum of the center of mass, and $\vec{p} = \frac{m_2\vec{p}_1 - m_1\vec{p}_2}{m_1+m_2}$ is the relative momentum. $\psi_{n_r l m_l}$ is the wave function for the bare meson state, with n_r being the radial quantum num

The Extended Friedrichs Scheme

The transition operator T in the QPC model for the $A \to BC$ process is defined as

$$\begin{aligned} T &= -3\gamma \sum_m \langle 1m1-m|00\rangle \int \mathrm{d}^3\vec{p_3}\mathrm{d}^3\vec{p_4}\delta^3(\vec{p_3}+\vec{p_4}) \\ & \mathcal{Y}_1^m(\tfrac{\vec{p_3}-\vec{p_4}}{2})\chi^{34}_{1-m}\phi^{34}_0\omega^{34}_0 b_3^\dagger(\vec{p_3})d_4^\dagger(\vec{p_4}), \end{aligned} \tag{16}$$

describing the process of a quark-antiquark pair being generated by the $b_3^\dagger$ and $d_4^\dagger$ creation operators from the vacuum. $\phi^{34}_0 = (u\bar{u}+d\bar{d}+s\bar{s})/\sqrt{3}$ is the $SU(3)$ flavor wave function for the quark-antiquark pair. χ^{34}_{1-m} and ω^{34}_0 are the spin wave function and the color wave function, respectively. $\mathcal{Y}_1^m$ is the solid Harmonic function. γ parameterizes the production strength of the quark-antiquark pair from the vacuum.

$X(3872)$

$\gamma \approx 4.0$

Table: Comparison of the experimental masses and the total widths (in MeV).

$n^{2s+1}L_J$	M_{expt}	Γ_{expt}	M_{BW}	Γ_{BW}	pole	GI
2^3P_2	3927.2 ± 2.6	24 ± 6	3920	10	3920-4i	3979
2^3P_1	3942 ± 9	37^{+27}_{-17}			3934-40i	3953
	3871.69 ± 0.17	< 1.2	3871	0	3871-0i	
2^3P_0	3862^{+66}_{-45}	201^{+242}_{-149}	3878	11	3878-5i	3917
2^1P_1			3895	37	3902-27i	3956

For $X(3872)$,
$Z_{c\bar{c}} : X_{\bar{D}^0 D^{0*}} : X_{D^+ D^{-*}} : X_{\bar{D}^* D^*} = 1 : (3.1 \sim 9.3) : (0.45 \sim 0.46) : 0.04$

$X(3872)$ wave function

wave function of the $X(3872)$ is expressed explicitly as

$$\begin{aligned}|X(3872)\rangle =& N_B\Big(|c\bar{c}\rangle + \int_{M_{00V}}^{\infty} \mathrm{d}E \sum_{S,L} \frac{f_{SL}^{00V}(E)}{z_X - E}(|E; D^0\bar{D}^{0*}, SL\rangle + |E; D^{0*}\bar{D}^0, SL\rangle) \\ &+ \int_{M_{+-V}}^{\infty} \mathrm{d}E \sum_{S,L} \frac{f_{SL}^{+-V}(E)}{z_X - E}(|E; D^+D^{-*}, SL\rangle + |E; D^{+*}D^-, SL\rangle) \\ &+ \int_{M_{0V0V}}^{\infty} \mathrm{d}E \sum_{S,L} \frac{f_{SL}^{0V0V}(E)}{z_X - E}|E; D^{0*}\bar{D}^{0*}, SL\rangle \\ &+ \int_{M_{+V-V}}^{\infty} \mathrm{d}E \sum_{S,L} \frac{f_{SL}^{+V-V}(E)}{z_X - E}|E; D^{+*}D^{-*}, SL\rangle\Big), \end{aligned} \tag{17}$$

where $N_B = \eta'(z_X)^{-1/2}$ is the normalization factor and z_X the mass of $X(3872)$.

The interaction Hamiltonian of the BS model in the coordinate space is

$$H_I = \sum_{ij}\left\{\frac{\alpha_s}{r_{ij}} - \frac{8\pi\alpha_s}{3m_i m_j}\vec{S}_i\cdot\vec{S}_j\delta(\vec{r}_{ij}) - \frac{3b}{4}r_{ij}\right\}\mathbf{F_i}\cdot\mathbf{F_j} \tag{18}$$

Barnes-Swanson Model

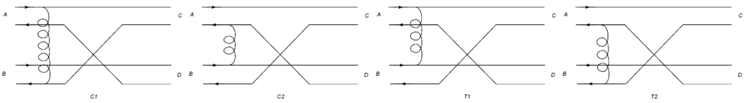

FIG. 2. The four quark rearrangement diagrams of $AB \to CD$ meson-meson scatterings. The arrows represent the quark line directions.

$X(3872) \to J/\psi\rho,\omega$

the branch fraction will be

$$\frac{\Gamma_{J/\psi\pi^+\pi^-\pi^0}}{\Gamma_{J/\psi\pi^+\pi^-}} = (3.24 \sim 2.43)^2 \times (0.088 \sim 0.098) = 0.92 \sim 0.58. \tag{19}$$

This numerical results are consistent with the measured ratio $1.0 \pm 0.4 \pm 0.3$ by Belle and 0.8 ± 0.3 by *BABAR*.

$X(3872) \to D^0 \bar{D}^{0*}$

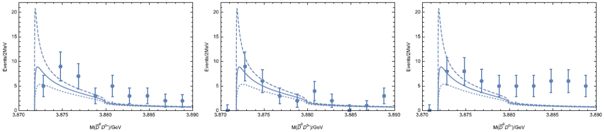

FIG. 4. The experimental $\bar{D}^0 D^{0*}$ mass distributions in $B \to X(\bar{D}^0 D^{0*})K$ decays of *BABAR* (left) [68] and Belle (middle and right) [67] compared with $r|T(\bar{D}^0 D^{0*} \to \bar{D}^0 D^{0*})|^2 \cdot phasespace$, where r is a rescaling factor chosen by hand. The dotted, solid, and dashed lines represent the curves with $X(3872)$ mass at 3.8710, 3.8714, and 3.8717 GeV, respectively.

Considering $\chi_{b1}(4P)$ and its coupling continua $B\bar{B}^*$ and $B^*\bar{B}^*$
Three zeros are found for $\eta^{nthsheet}(E) = 0$

$$\begin{aligned} z_v &= 10593MeV, (virtual\ state) \\ z_{R1} &= 10771 \pm 3iMeV, \\ z_{R2} &= 10672 \pm 39iMeV. \end{aligned} \tag{20}$$

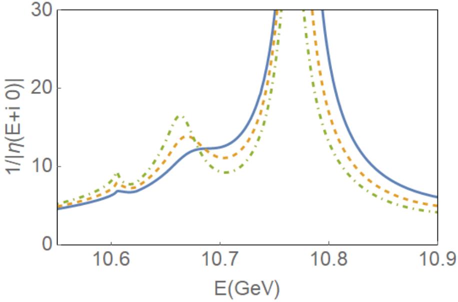

Poles' trajectories

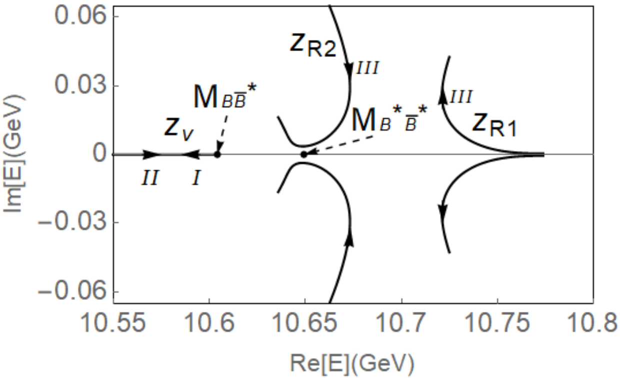

Figure: The trajectories of poles as γ increases. The I, II, and III denote the sheet numbers of the poles as described in the text. z_v, z_{R1}, and z_{R2} with both $B\bar{B}^*$ and $B^*\bar{B}^*$ continua.

Poles' trajectories

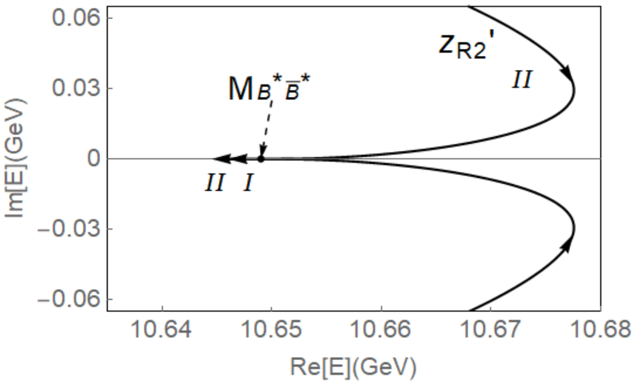

Figure: The trajectories of poles as γ increases. The I, II, and III denote the sheet numbers of the poles as described in the text. z'_{R2} poles with only the $B^*\bar{B}^*$.

The Residue Functions and Scattering Amplitudes

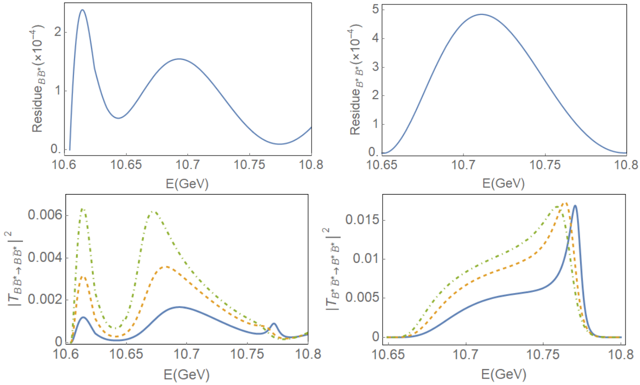

Figure: The residue functions of $B\bar{B}^*$(left) and $B^*\bar{B}^*$(right) are shown in the first row. The absolute square of scattering amplitudes of $B\bar{B}^*$ and $B^*\bar{B}^*$ with $\gamma = 4.0$(solid), 4.9(dashed), and 5.6(dotdashed), respectively, are shown in the second row.

How to understand experiment results?

In this picture, the absence of the X_b signal in $\Upsilon\pi\pi$ channel by CMS and in $\Upsilon\pi\pi\pi$ in Belle can be explained. Both channels are OZI suppressed. If we suppose that the three pions come from ω and the lower $\Upsilon\omega$ channel is open but coupled weakly, the second sheet virtual pole will move to the third and fourth sheets, with its mass below the $B\bar{B}^*$ threshold, which would not affect $1/|\eta|$ significantly in the physical region which is attached to the second sheet below the $B\bar{B}^*$ threshold and to the third sheet above the threshold. The residue function of $\chi_{b1}(4P)$ to $\Upsilon\omega$ is OZI suppressed and thus any structure would not be easily observed. So, We suggest further experimental search is paid more attention to the $B\bar{B}^*$ channel, which could be achieved when the SuperKeKB energy is increased.

Summary

- The Extended Friedrichs Scheme might shed more light on hadron physics.
- X_b is a virtual state, so the signal in $\Upsilon(1S)\omega$ is not easy to extract.
- A lineshape peak at about 10615 MeV with a width about 10 MeV above $B\bar{B}^*$ threshold is predicted. It could be regarded as X_b but it main comes from the convolution of wave functions.
- Another dynamically generated state at about $10672 \pm 39i$ MeV
- The physical $\chi_{b1}(4P)$ is at about $10771 \pm 3i$ MeV

Thanks for your patience!

Extra slides

Extra slides